

Steady swimming muscle dynamics in the leopard shark *Triakis semifasciata*

Jeanine M. Donley* and Robert E. Shadwick

Marine Biology Research Division, Scripps Institution of Oceanography, University of California, San Diego,
La Jolla, CA 92093-0202, USA

*Author for correspondence (e-mail: jdonley@ucsd.edu)

Accepted 23 December 2002

Summary

Patterns of red muscle strain and activation were examined at three positions along the body (0.42, 0.61 and 0.72L, where L is total body length) and correlated with simultaneous measurements of midline kinematics during steady swimming (approx. 1.0 L s^{-1}) in the leopard shark *Triakis semifasciata*. Analysis of lateral displacement along the body indicates that the leopard shark is a subcarangiform swimmer. Longitudinal variation in red muscle strain was observed with strain amplitudes ranging from $\pm 3.9\%$ in the anterior, $\pm 6.6\%$ in the mid, to $\pm 4.8\%$ in the posterior body position. Strain was in-phase with local midline curvature. In addition, strain amplitude calculated from a bending beam model closely matched strain measured using sonomicrometry at all three body positions. There is a high degree of similarity in red muscle activation patterns along the body between the leopard shark and many fish species, in that the onset of

activation occurs during muscle lengthening while offset occurs during muscle shortening. However, we found no significant longitudinal variation in the EMG/strain phase relationship and duty cycles, with onset of muscle activation occurring at $51.4\text{--}61.8^\circ$ and offset at $159.7\text{--}165.2^\circ$ (90° is peak length). This consistent pattern of activation suggests that red muscle along the entire length of the body contributes to positive power production. Thus, sharks such as *Triakis* may have no regional specialization in red muscle function like that seen in many teleosts, which may indicate that the evolution of differential muscle function along the body occurred after the divergence of cartilaginous and bony fishes.

Key words: muscle activation, muscle strain, electromyography, sonomicrometry, shark, *Triakis semifasciata*.

Introduction

One of the most conspicuous features of the locomotor muscle in fish is the distinct segregation of two functionally different fiber types: red oxidative and white glycolytic. In most bony and cartilaginous fishes, the red muscle comprises a thin subcutaneous wedge or sheet of muscle that is located near the lateral line while the white muscle comprises the bulk of the body cross-section. Some of the earliest research on the function of muscle in swimming fish focused on identifying the role of the red and white fibers in various swimming behaviors in sharks. Using electromyography (EMG), Bone (1966) showed that in dogfish shark the red muscle fibers were active during slow, steady swimming whereas white fibers were active when high burst speeds were required. Given differences in mitochondrial content, fat and glycogen content, patterns of innervation, and EMG activity at various swimming speeds between the two fiber types, Bone (1966) concluded that the red and white muscle in dogfish represent two distinct motor systems which operate independently. Following this work, the focus of studies investigating the function of fish muscle during swimming shifted from sharks to bony fishes. Indeed, the same pattern of differential muscle function between red and white fibers was shown in teleosts. Only red muscle was found to be

active at slow swimming speeds, whereas white muscle was shown to be active only at burst speeds (Rayner and Keenan, 1967), or at progressive levels of recruitment starting at the upper range of sustainable swimming speeds (Greer-Walker, 1970; Johnston and Goldspink, 1973a,b; Johnston et al., 1977; Bone et al., 1978; Hochachka et al., 1978).

In addition to examining the roles of the two major muscle fiber types as a function of swimming speed, numerous studies have investigated the timing of red muscle activation at different positions along the body during steady swimming. When superficial red muscle is active it contracts to produce local bending of the body, and the wave of lateral motion that generates thrust is the summation of the sequential muscle contractions along the body. Common features of activation patterns during steady swimming among several teleost species are that the wave of red muscle activation travels (1) down the body in a rostrocaudal direction (Grillner and Kashin, 1976; Williams et al., 1989; He et al., 1990; van Leeuwen et al., 1990; Jayne and Lauder, 1993, 1995b; Gillis, 1998; Knower et al., 1999; Shadwick et al., 1999) and (2) faster than the propulsive wave of lateral displacement (Grillner and Kashin, 1976; Wardle et al., 1995; Katz and Shadwick, 1998).

Because the wave of muscle activation travels down the body faster than the wave of lateral displacement, the phase of the muscle length change (strain) cycle in which red muscle is active also varies along the body. This observation led to research that focused on quantifying red muscle activity and shortening at different axial positions; specifically, studies examined the EMG/strain phase relationship. A common trend that has emerged among teleosts is that red muscle activation typically occurs during muscle lengthening (from 0 to 90° of the strain cycle) and offset occurs during muscle shortening (typically 100–250°) (Altringham and Ellerby, 1999). This pattern enhances positive power production in cyclic contractions of fish muscle (Altringham and Johnston, 1990). In addition, in many teleosts there is a decrease in the duration of muscle activation towards the tail, a shift in the EMG/strain phase at more posterior locations such that onset occurs relatively earlier in the strain cycle (Williams et al., 1989; van Leeuwen et al., 1990; Rome et al., 1993; Wardle and Videler, 1993; Jayne and Lauder, 1995b; Hammond et al., 1998; Shadwick et al., 1998; Ellerby and Altringham, 2001; Knower et al., 1999), and a rostrocaudal increase in strain amplitude.

The importance of the longitudinal variation in the EMG/strain phase relationship is that the timing of activation of a muscle relative to its lengthening and shortening cycle, and the duration of muscle activation, affect the net work produced and thus its mechanical contribution to swimming, as has been shown in recent *in vitro* work loop studies. In some fish species, the anterior musculature is hypothesized to produce the majority of the power for thrust (van Leeuwen et al., 1990; Altringham et al., 1993; Wardle and Videler, 1993), whereas in other species the posterior musculature is mainly responsible for thrust production (Coughlin and Rome, 1996; Rome et al., 1993; Johnson et al., 1994; Jayne and Lauder, 1995b). Some fish species display a relatively constant pattern of power production along the body (Shadwick et al., 1998; Ellerby et al., 2000; Syme and Shadwick, 2002; D'Aout et al., 2001).

The main conclusions to be drawn from recent studies are that dynamic muscle function varies longitudinally in many bony fishes and that different species exhibit various patterns of muscle activation and strain in order to optimize muscle function for their particular swimming behavior. Optimization of muscle function along the body may be correlated with differences in swimming mode (Wardle et al., 1995). Since the earliest research on muscle function in fish swimming, attention has been focused on bony fishes representing a wide range of swimming modes. However, sharks also display a broad spectrum of swimming modes, ranging from highly undulatory species (large lateral displacement over much of the body) such as the leopard shark, to more stiff-bodied, tuna-like species (lateral displacement restricted primarily to caudal region) such as the lamnid sharks, yet virtually nothing is known about dynamic muscle function in any shark species. To build a more complete picture of the evolution of muscle function in fish swimming it is important to address the following questions with respect to sharks: (1) which features

of the muscle dynamics found in teleosts also occur in sharks, (2) are there any regional variations in patterns of muscle strain and activation in sharks as seen in teleosts, and (3) are there differences in the muscle dynamics of sharks that have different swimming modes? The present study addresses the first two questions by examining the *in vivo* muscle dynamics of the leopard shark *Triakis semifasciata* and comparing muscle function in this coastal shark species with data that exist on bony fishes. Specific objectives are to (1) characterize the patterns of muscle strain at different axial positions, (2) compare the timing of red muscle activation relative to the phase of the strain cycle at different axial positions, (3) determine if longitudinal differences in EMG duration occur and (4) compare measured strain to strain predicted from midline curvature derived from analysis of the kinematics during steady swimming.

Materials and methods

Experimental animals

Eleven leopard sharks *Triakis semifasciata* (Girard), ranging in size from 70.5 to 96.3 cm total length (L), were collected by gill net and hook-and-line off the coast of Southern California and transported to the Scripps Institution of Oceanography (SIO) in a 380 liter bait tank. At SIO, the specimens were kept in a 3 m diameter tank with a continuous flow of seawater and aeration within a temperature range of 14–16°C. They were fed squid and chopped fish weekly until satiated. The sharks were allowed to acclimate to their new surroundings for a minimum of 2 weeks prior to experimentation. Only healthy individuals were used in the experiments. All procedures in capture, maintenance and experimentation followed the guidelines of our University of California, San Diego (UCSD) animal care protocol.

Surgical procedures

Surgery was performed to implant piezoelectric crystals and EMG electrodes into the red muscle of each leopard shark for *in vivo* detection of muscle strain and activation patterns. Prior to surgery, the fish were submerged in seawater containing anesthetic (0.0139 g l⁻¹ ethyl *p*-aminobenzoate) and remained anesthetized typically for 30 min, but for no more than 60 min, throughout the procedure by recirculation of the anesthetic across the gill surfaces. Following surgery, the fish were allowed to recover in fresh seawater and placed into the swim tunnel to become acclimated to the test chamber prior to data collection.

Sonomicsrometry

Pairs of 2 mm barrel piezoelectric ceramic crystals (Sonometrics Corp., Ontario, Canada), one acting as an acoustic transmitter and the other as a receiver, were first calibrated in seawater and then implanted using a 13-gauge hypodermic needle at three axial positions (0.42±0.024 L , 0.61±0.02 L and 0.72±0.023 L) (Fig. 1). Pairs of crystals were implanted into the subcutaneous red muscle parallel to each

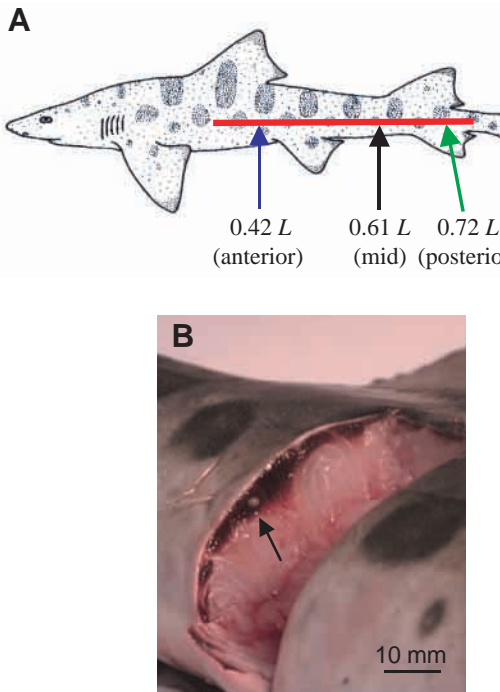


Fig. 1. (A) Leopard shark image modified from Miller and Lea (1972). The red bar represents the longitudinal range of red muscle and the arrows indicate the three axial positions examined in this study. (B) Post-mortem dissection showing the lateral band of red muscle at $0.42L$ and placement of a sonometric crystal (indicated by the arrow).

other just ventral to the lateral line on the left side of the body. The crystals were implanted perpendicular to the longitudinal axis of the body, so the bending movements of the shark would not cause slippage of the crystals within the muscle or prevent restriction of movement of the crystal head. They were implanted at the same depth within the muscle (2.0 mm) to avoid miscalculation of changes in muscle length. The proper position and orientation of the crystals was maintained by anchoring the crystal wires to the skin in several locations along the left side of the body and along the dorsal surface with sutures and Vetbond tissue adhesive. The wires were then bundled together to prevent tangling. Sonometric data were collected digitally at a frequency of 500 Hz during periods of steady swimming when the shark was positioned in the center of the flow chamber. At the end of each experiment, crystal depth and body width at implantation sites was recorded. Sonometric data were filtered in AcqKnowledge 3.5 (Biopac Systems Inc.) using a Blackman-92db FIR 60 Hz band stop filter. This filter removed from the sonometric data the electrical noise produced by the swim tunnel motor.

Electromyography

During the surgery for sonomicrometry, EMG electrodes were implanted into the red muscle approximately 1–2 mm apart at the same depth and axial position as the sonometric crystals. The electrode wires were anchored to the skin with

sutures and tissue adhesive and bundled together with the crystal wires. EMG signals were amplified using a.c. preamplifiers (Grass Instrument Co., West Warwick, USA), band-pass filtered (3–1000 Hz), and recorded simultaneously with the sonometric data at 500 Hz. With a sample frequency of 500 Hz and a typical tailbeat period of 1 Hz, the error in EMG timing did not exceed 2 ms or an error of 0.2% of one cycle.

Analysis of sonometric and EMG data

Selection criteria

In order to select a series of tailbeat cycles for analysis, the following criteria were established: (1) the data must correspond to periods when the shark swam for 10 or more consecutive complete tailbeat cycles in the center of the chamber, and (2) the EMG traces must display a signal in which the onset and offset of EMG activity were discernible. Because of difficulty in eliminating all sources of electrical noise during data collection, some of the sonometric and EMG data traces were not adequate for analysis. Therefore, EMG data for the anterior position ($0.42L$) are presented for eight individuals, for the mid body position ($0.61L$) for nine individuals, and for the posterior position ($0.72L$) for four individuals. Sonometric data for the anterior and mid body positions are presented for nine individuals, and for the most posterior location for four individuals.

Muscle strain

Muscle strain was calculated from the muscle length traces recorded during steady swimming. Muscle strain amplitude was calculated by subtracting the mean muscle length from the peak of the waveform and dividing this difference by mean length.

EMG/strain phase and EMG duration

The muscle strain waveform was periodic and therefore the phase of the strain cycle was designated in degrees (from 0 to 360), the start of each strain cycle (0°) being the point at which mean muscle length was achieved during lengthening (see Altringham and Johnston, 1990). Using AcqKnowledge 3.5 (Biopac Systems Inc.), EMG traces were filtered with a Blackman-92 db FIR high-pass filter with a cut-off frequency of 3 Hz (to remove low-frequency movement artefact) and a 60 Hz band stop filter to remove the electrical noise created by the swim tunnel motor. Timing of onset and offset of activation were determined using a voltage threshold method described in Knower et al. (1999). The temporal relationships between onset and offset of activation and the muscle strain cycle were expressed in degrees. The duration of muscle activation was calculated from the onset and offset times for each tailbeat cycle. EMG/strain phase and EMG duration data presented in this paper represent an average of multiple tailbeat cycles for each fish. Fig. 2 illustrates one complete strain cycle with the corresponding EMG trace; the vertical lines in Fig. 2B indicate the positions at which onset and offset of activation occurred.

Kinematic analysis

Concurrent with measurements of instantaneous muscle length changes and EMG activity, each individual was videotaped at 60 Hz with a Canon Inc. digital camera (model XL1) while swimming against a current of known velocity in a swim tunnel. The variable-speed swim tunnel used in these experiments has been described in Graham et al. (1990). When the fish maintained its position in the flow chamber, its swimming speed was determined from the speed of the current inside the chamber. To synchronize the collection of sonometric, EMG and video recordings, a flashing red diode was recorded in the video sequences and its excitation voltage was recorded with the sonometric and EMG data.

The camera was positioned approximately 1 m directly above the working section of the swim tunnel to obtain a dorsal view of the fish (Fig. 3). Video recordings were made over a 10–45 min period at a speed of approximately 1.0 L s^{-1} (total body lengths s^{-1}). Video segments in which the fish completed four or more symmetrical tailbeats near the center of the chamber and that corresponded to acceptable strain and EMG data for all axial locations were selected for kinematic analysis.

The purpose of the kinematic analyses was to correlate patterns of body bending captured on videotape with measurements of local muscle activation and strain. 32 equally spaced points along the dorsal outline were digitized in sequential video fields using Scion Image (Scion Corporation, www.scioncorp.com). Dorsal outlines were confined to the mid and posterior regions of each fish, beginning anteriorly at the trailing edge of the pectorals (approx. $0.3L$) and ending at the tip of the caudal fin. A scaling factor was calculated for each video sequence using a 10 cm grid on the bottom of the chamber.

A cubic spline function was used to convert the point coordinate data of each digitized outline into complete curves (see Jayne and Lauder, 1995a). A dorsal midline for each field was then calculated using a computer algorithm and this midline was divided into 50 equally spaced segments. The progression of these points in the y-direction (perpendicular to axis of progression of the fish) was used to calculate lateral amplitude along the body through a series of consecutive tailbeat cycles. Lateral displacement was defined as the peak-to-peak lateral amplitude divided by two. A mean value was calculated from four consecutive tailbeat cycles in nine fish. To allow for comparison of individuals of different sizes, lateral displacements were expressed in units relative to body length (% L).

Propulsive wave velocity C , defined as the speed of the wave of lateral motion that travels along the body rostrocaudally, was calculated from the lateral displacement data by dividing the distance between two designated points on the body, the anteriormost position observed in consecutive video frames ($0.3L$) and the tip of the caudal fin, by the time between peaks of lateral motion at these two axial positions. Propulsive wavelength (λ) was then calculated as C divided by mean tailbeat frequency (tbfs).

Curvature

Using the point coordinate data of the dorsal midline, curvature was calculated as described in van Leeuwen et al. (1990), Rome et al. (1992), Coughlin et al. (1996) and Katz and Shadwick (1998). The fish body was treated as a dynamic bending beam in which the bending of segments along the body was correlated with the local shortening of the red muscle. Midline coordinate data were normalized in the x -

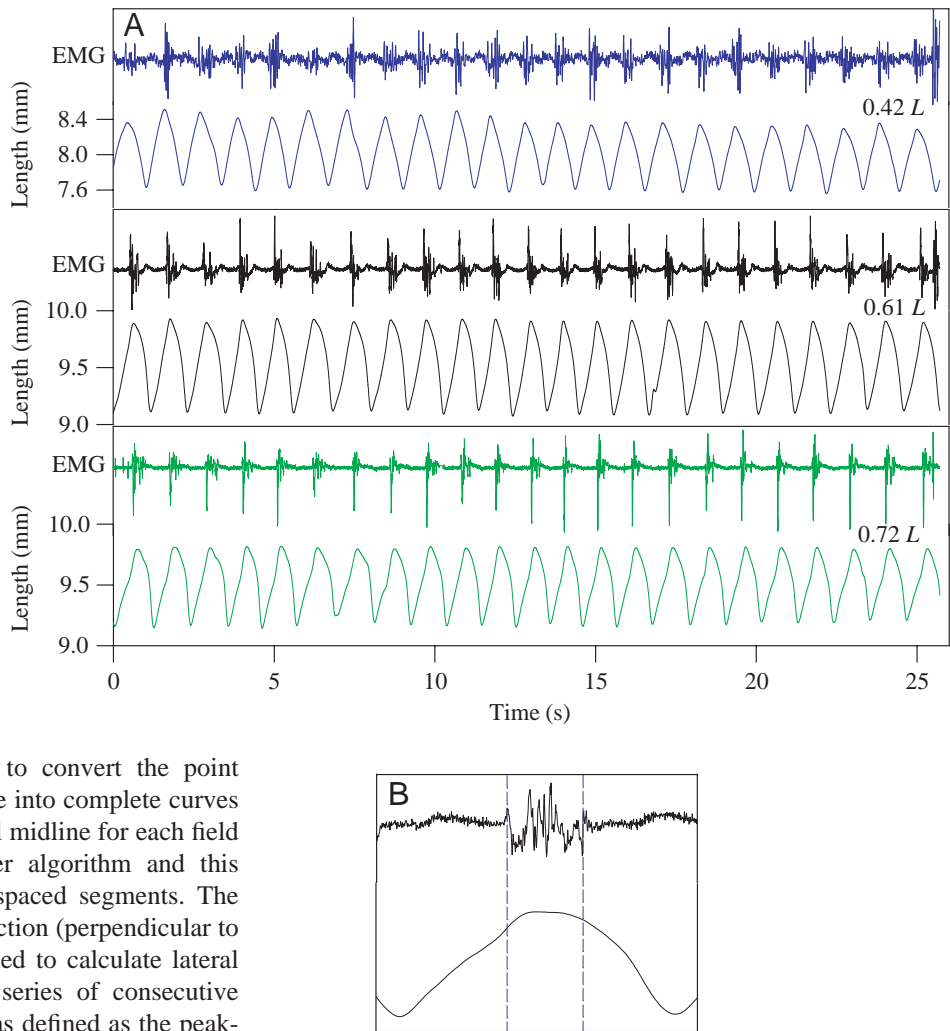


Fig. 2. (A) An example of electromyographic (EMG) and sonometric traces recorded simultaneously over several consecutive tailbeat cycles at three axial positions in an 88.0 cm leopard shark. (B) Close-up of one tailbeat cycle. Vertical lines indicate onset and offset of EMG activity.

direction (defined by the direction of travel) and a fourth order polynomial equation was fitted to each midline (see Katz and Shadwick, 1998). r^2 values ranged from 0.98000 to 0.99999. Curvature K , defined as the inverse of the radius of curvature, was calculated from the polynomial equations for several positions along the dorsal midline ($0.4L$, $0.5L$, $0.6L$, $0.7L$, $0.8L$ and $0.9L$) in nine individuals using the following equation:

$$K(x) = z''(x)/\{1+[z'(x)]^2\}^{3/2}, \quad (1)$$

where $z(x)$ describes the fish midline in coordinate space. This equation differentiates $z(x)$ with respect to x to obtain curvature. Predicted strain values were calculated from curvature at the anterior, mid and posterior positions by multiplying the curvature at each position in each frame by the distance between the crystals and the backbone (van Leeuwen et al., 1990; Rome et al., 1992, 1993; Coughlin et al., 1996; Katz and Shadwick, 1998).

Statistics

Muscle dynamics

We investigated whether or not there was a significant difference among the different body positions examined in terms of the degree of muscle strain, the timing of onset and offset of activation, and duty cycle. Because these parameters may vary both with position and among the individuals, a multivariate analysis of variance (MANOVA) was performed in order to assess the effects of position, individual and a position/individual interaction. In addition, when individual effects were significant, an analysis of variance (ANOVA) was performed on each individual in order to determine whether the position effects were significant. A Tukey-Kramer pairwise comparisons analysis was performed to identify specific differences in mean strain, the timing of onset and offset of activation, and duty cycle between the three different body positions.

Kinematics

The lateral displacement data were examined using a MANOVA to determine whether there were any significant effects of body position, individual or position/individual interactions. To examine the relationship between strain values predicted from calculations of midline curvature and those values measured using sonomicrometry, these data were also subjected to analysis of variance with position and individual effects incorporated into the statistical model. All statistical analyses were performed in Minitab (version 13) using a significance level of $P=0.05$.

Results

Patterns in muscle shortening

Results presented in this paper correspond to data collected at the preferred swimming speed of the sharks, which was approx. $1.0 L s^{-1}$. Mean muscle strain

amplitudes were $\pm 3.9\%$ in the anterior, $\pm 6.6\%$ in mid, and $\pm 4.8\%$ in the posterior (Fig. 4, Table 1). Statistical results indicated that both position and individual effects were significant ($P<0.001$). In order to remove the effect of individual variation from the statistical model and simply determine whether the longitudinal variation in strain was similar in all sharks, an ANOVA was performed on the strain data for each individual. The results from this test verified the results from the full multivariate model and indicated that the effect of position was significant in all sharks ($P<0.050$). Tukey's pairwise comparisons analysis showed a significant difference between strain at all three body positions, with the greatest strain values occurring in the mid body position in all individuals examined.

Patterns in muscle activation

The timing of muscle activation was expressed in degrees relative to the phase of the strain cycle, and duty cycle, defined as the time in which the muscle was activated relative to the total time of the strain cycle, was expressed as a percentage. At all three axial positions onset of activation occurred during muscle lengthening and offset occurred during muscle shortening (Fig. 5). Mean onset of activation occurred at 54.2° in the anterior, 51.4° in mid and 61.8° in the posterior positions. Mean offset of activation occurred at 165.2° in the

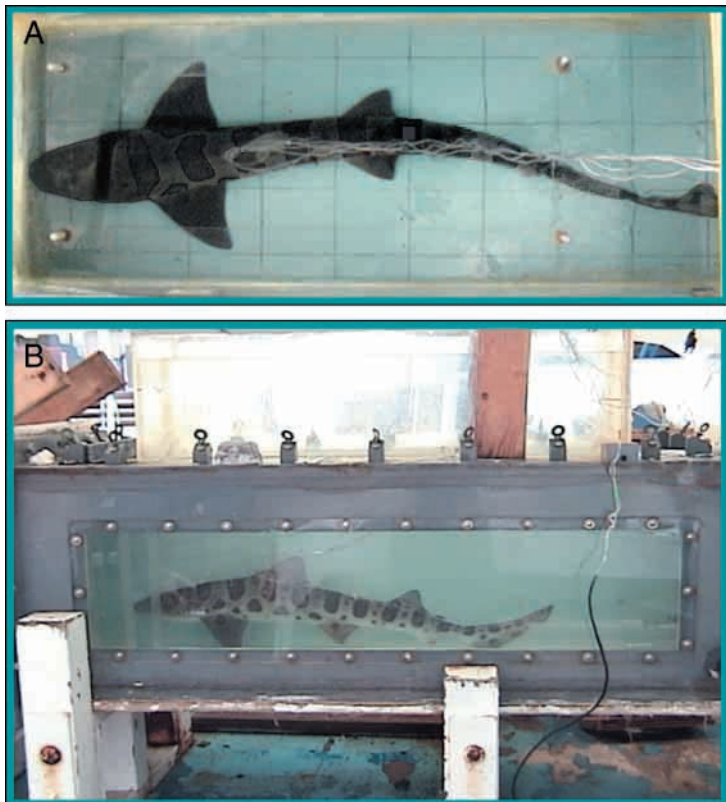


Fig. 3. Dorsal view (A) and lateral view (B) of a 94.5 cm leopard shark swimming in the swim tunnel. Dorsal images were obtained during steady swimming concurrent with sonometric and EMG recordings in order to correlate midline kinematics with measurements of red muscle strain and activation.

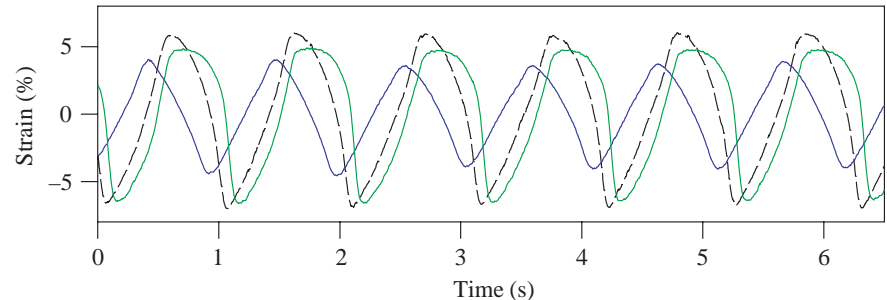


Fig. 4. An example of red muscle strain measured over six consecutive tailbeat cycles in the anterior (blue), mid (black), and posterior (green) positions in a 77.0 cm leopard shark. Strain amplitudes varied significantly between the three body positions ($P < 0.050$) in all sharks examined.

Table 1. Mean muscle strain and activation phase in leopard sharks swimming at approx. 1.0 L s^{-1}

Body position	Strain (%)	EMG onset (degrees)	EMG offset (degrees)	Duty cycle (%)
$0.42 \pm 0.024 L$	$\pm 3.9 \pm 0.3$ (8)	54.2 ± 4.4 (8)	165.2 ± 5.5 (8)	30.9 ± 1.5 (8)
$0.61 \pm 0.02 L$	$\pm 6.6 \pm 0.2$ (8)	51.4 ± 3.2 (9)	163.1 ± 5.9 (9)	31.0 ± 1.4 (9)
$0.72 \pm 0.023 L$	$\pm 4.8 \pm 0.4$ (4)	61.8 ± 4.4 (4)	159.7 ± 9.4 (4)	25.8 ± 2.8 (4)

Values are means \pm S.E.M. representing variation among leopard shark individuals; sample sizes are in parentheses.

anterior, 163.1° in mid and 159.7° in the posterior positions (Table 1). Duty cycles were 30.9% in the anterior, 31.0% in mid and 25.8% in the posterior positions.

In order to identify longitudinal variation in the timing of muscle activation, as with the analysis of the strain data, these data were subjected to a MANOVA using position, individual and position/individual interaction as the parameters in the statistical model. Statistical analysis indicated that there was no significant effect of body position ($P > 0.050$) in both the onset and offset of activation as well as the duty cycle. There was a significant variation among individuals, however, so an additional analysis was performed. In order to remove the effect of individual variation from the statistical model and simply determine whether the timing of muscle activation was similar along the body in all sharks, an ANOVA was performed on the EMG/strain phase and duty cycle data for each individual. After removing the confounding effects of individual variation from the statistical model, there remained no significant longitudinal variation in the onset and offset of activation ($P > 0.050$). Mean duty cycles were also statistically similar at all three body positions ($P > 0.050$).

Lateral displacement

Kinematic analysis was performed on nine leopard sharks in which mean lateral displacement of the dorsal midline was calculated for each fish over a series of approximately five tailbeat cycles. Lateral displacement D was expressed as a percentage of total body length (% L). Position along the body was represented as a fraction of total length L . Displacement data were collected for positions along the body between $0.3L$ and $1.0L$. Lateral displacement varied significantly ($P < 0.001$) with axial position and ranged from 1.43 ± 0.22 at $0.3L$ to 9.95 ± 0.87 at $1.0L$. D increased rapidly over the posterior half

of the body, reaching a maximum at the tip of the caudal fin (Fig. 6).

Propulsive wave velocity and wave length

Average propulsive wave velocity C was lower than the speed of the wave of muscle strain (Table 2). Propulsive

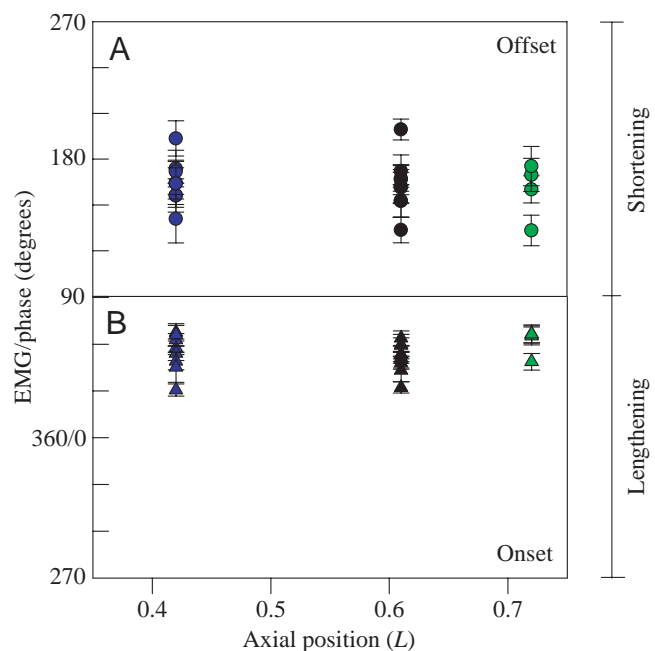


Fig. 5. Timing of muscle activation at three axial positions. Offset of activation (A) occurred during muscle shortening and onset (B) occurred during muscle lengthening at all positions in all leopard sharks examined. There was no significant longitudinal variation in the phase of activation in all individuals examined. Values are means \pm S.D. calculated for several tailbeat cycles in each fish.

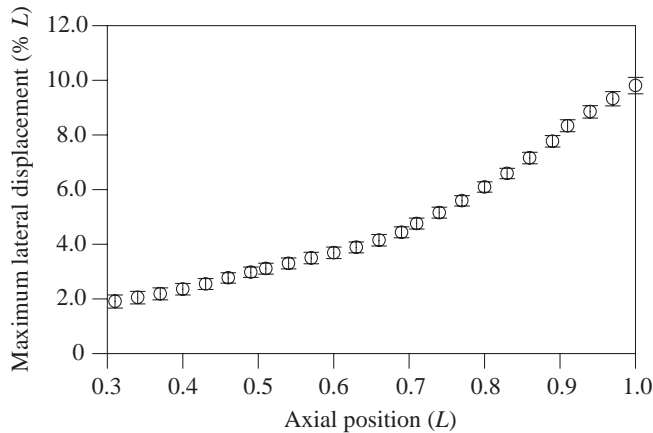


Fig. 6. Maximum lateral displacement (% L) of the dorsal midline as a function of body position. Values represent mean \pm S.E.M. of maximum displacement for nine leopard sharks swimming at 1.0 L s^{-1} . Lateral displacement was greatest at the tip of the caudal fin.

wavelength λ was shorter than body length in all individuals, indicating that more than one propulsive wave was traveling along the body at any point in time, a result similar to those shown for *Triakis* in previous studies (Webb and Keyes, 1982).

Muscle shortening in relation to body curvature and predicted strain

Curvature as a function of time was calculated at several positions along the dorsal midline, including those corresponding to the locations of implanted crystals and electrodes. A comparison between the midline curvature and muscle strain at a given point in time revealed that red muscle shortening at all three body positions ($0.42L$, $0.61L$ and $0.72L$) closely matched the phase of local midline curvature (Fig. 7).

Predicted strain values were calculated from curvature by multiplying the curvature by the distance between the crystals and the backbone. There was no significant difference between strain measured by sonomicrometry and strain predicted from midline curvature ($P>0.050$) at all three body positions ($N=3$).

Table 2. Kinematic parameters calculated from analysis of video footage recorded during steady swimming in four leopard sharks

L (cm)	Prop-wave velocity C (cm s^{-1})	Propulsive wavelength λ (% L)	Tailbeat frequency (Hz)	Velocity of wave of muscle strain (cm s^{-1})
94.5	96.7	95.7	1.07	125.8
70.5	57.0	94.8	0.85	83.5
84.0	62.1	51.7	1.43	149.5
77.5	66.3	72.5	1.18	116.0

L , total body length; C , propulsive wave velocity; λ , propulsive wavelength.

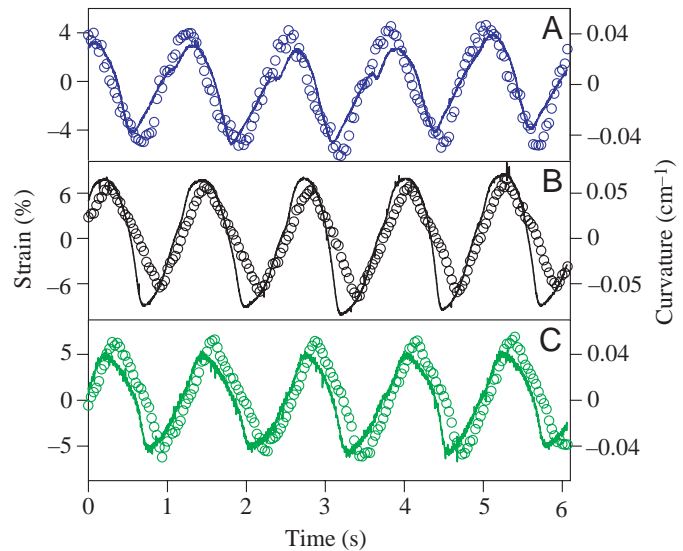


Fig. 7. Red muscle strain (solid line) measured by sonomicrometry superimposed onto predicted strain (open circles) calculated from midline curvature for five tailbeat cycles at three body positions, anterior (A), mid (B) and posterior (C), in a 94.5 cm leopard shark, to illustrate the similarity between values of predicted and measured strain. The phase of measured strain closely matched the phase of local midline curvature (open circles, right axis), and thus predicted strain at all body positions in all individuals examined.

Discussion

This study investigated the simultaneous patterns of *in vivo* red muscle strain and activation along with aspects of the midline kinematics in a common coastal shark species, the leopard shark *Triakis semifasciata*.

Lateral displacement

Comparison of the lateral displacement as a function of body position between the leopard shark and various bony fishes indicates that the leopard shark is not an anguilliform swimmer (e.g. Lindsay, 1978), but rather swims with a subcarangiform mode of locomotion that is intermediate between anguilliform (e.g. eel) and carangiform (e.g. mackerel), and characterized by displacement amplitudes that increase rapidly over the posterior half of the body (Webb, 1975). For example, lateral displacement increases from 2.8% at $0.5L$ to 9.9% at $1.0L$ (Fig. 6). Furthermore, the displacement at $0.5L$ in the leopard shark is approximately half that in the eel and double that observed in a mackerel (see fig. 2 in Altringham and Shadwick, 2001). A similar conclusion was reached by Webb and Keyes (1982), who examined the kinematics of six species of free-swimming sharks, including *Triakis*, and showed that patterns of undulation and the approximate number of propulsive waves on the body at a given time were consistent with a subcarangiform mode of locomotion.

Muscle shortening in relation to body curvature and predicted strain

Dorsal midline curvature has been shown to provide an

accurate approximation of strain in teleosts with superficial red muscle (Coughlin et al., 1996; Shadwick et al., 1998; Katz et al., 1999). A comparison between the midline curvature and muscle length as a function of time revealed that red muscle shortening is in-phase with local curvature in the leopard shark (Fig. 7). Synchronization between muscle length changes and curvature indicates that red muscle contractions are responsible for local bending of the body, a result consistent with observations in teleosts with red muscle closely associated with the skin. In addition, strain amplitude calculated from a bending beam model closely matched strain measured at three body positions (Fig. 7).

Muscle strain

Red muscle strain amplitudes observed in the leopard shark were similar in magnitude to those observed in previous studies of teleosts. Strain varied from $\pm 3.9\%$ in the anterior to $\pm 6.6\%$ in mid and $\pm 4.8\%$ in the posterior position (Fig. 4; Table 1). Hammond et al. (1998) described strains of 3.3% at $0.35L$ and 6.0% at $0.65L$ in rainbow trout. These values are similar to those observed in saithe (Hess and Videler, 1984), carp (van Leeuwen et al., 1990), scup (Rome and Swank, 1992; Rome et al., 1993), mackerel (Shadwick et al., 1998) and bonito (Ellerby et al., 2000).

A trend commonly observed in teleosts is an increase in red muscle strain from anterior to posterior, generally corresponding to an increase in lateral displacement along the body (Hess and Videler, 1984; Rome et al., 1990, 1993; Coughlin et al., 1996; Knower et al., 1998; Shadwick et al., 1999). Similar to teleosts, the leopard shark also displays an increase in strain from the anterior to mid body region; however, unlike many fishes, the tapering of the body leads to a decline in strain amplitude at $0.7L$. From $0.6L$ to $0.7L$, body thickness decreases, but curvature is similar at both positions, leading to a small decrease in predicted and measured strain at $0.7L$ (see Figs 7 and 8). This decrease in strain near $0.7L$ may simply be a consequence of the high degree of tapering along much of the body that is seen in elongated fishes (e.g. European eel; D'Aout and Aerts, 1999) as opposed to fishes with tapering confined largely to the peduncular region.

Patterns of red muscle activation

There is a high degree of similarity in red muscle activation patterns along the body between the leopard shark and many fish species, in that the onset of activation typically occurs late in the lengthening phase, while offset occurs during muscle shortening. This activation pattern ensures that muscle develops high force near peak length and actively shortens to produce positive contractile work, and it is a requirement for optimizing power production during steady swimming (Altringham and Johnston, 1990).

In vitro work-loop studies have verified the difference in net work produced by muscles operating under different patterns of strain and activation. Recent *in vitro* work-loop studies approximating *in vivo* patterns of strain and activation have revealed different trends in muscle function among fishes. In

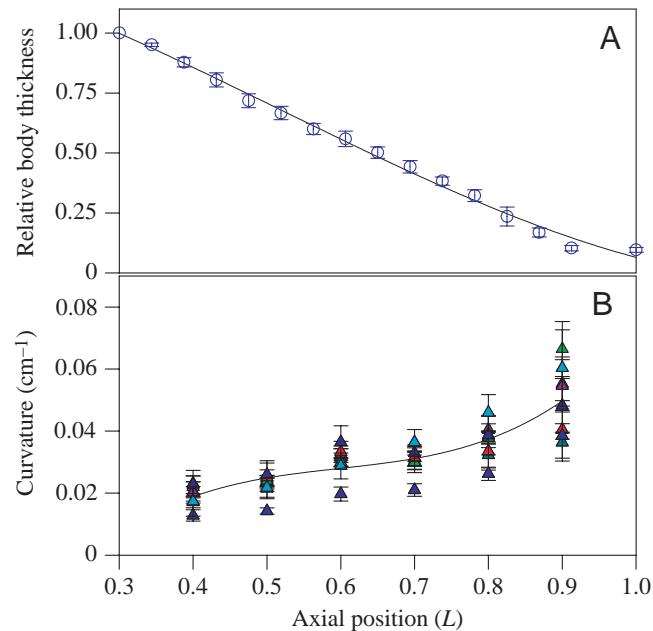


Fig. 8. (A) Relative body thickness (mean \pm S.E.M.) of five leopard sharks as a function of axial position. To compare individuals of different sizes, body thickness is normalized to thickness measured at $0.3L$. Thickness measurements were made from dorsal video images. (B) Dorsal midline curvature calculated for six positions along the body in eight leopard sharks swimming $1.0Ls^{-1}$. Values are means \pm S.D. calculated from four tailbeat cycles for each fish at each body position.

some species there is little longitudinal variation in muscle power output (Syme and Shadwick, 2002). Conversely, other fish species have been shown to produce net positive work at both anterior and posterior body positions (Coughlin and Rome, 1996; Rome et al., 1993; Johnson et al., 1994). Because the amplitude of strain is greater in the posterior region, it was suggested in these studies that power production originates mainly from the posterior musculature. A third trend is that the anterior musculature has a greater net positive work (muscles activated predominantly during shortening) than the posterior musculature and thus produces the majority of power for thrust production (van Leeuwen et al., 1990; Altringham et al., 1993; Wardle and Videler, 1993; Hammond et al., 1998). Regardless of the pattern of power production, the situation where posterior muscles are being lengthened while active during a portion of the time in which the anterior muscle is actively shortening probably occurs because of the time delay that accompanies the wave of contraction traveling along the body. For example, in saithe peak power in the anterior portion of the body occurred while the rear muscles were lengthening and developing peak force (Altringham et al., 1993). In the leopard shark, a portion of the EMG/strain cycle producing positive work in the anterior region occurred simultaneously with active lengthening in the mid and posterior musculature (Fig. 9). Stiffening of the posterior musculature (due to active lengthening) concurrent with positive power production by the anterior musculature may affect the transmission of the wave

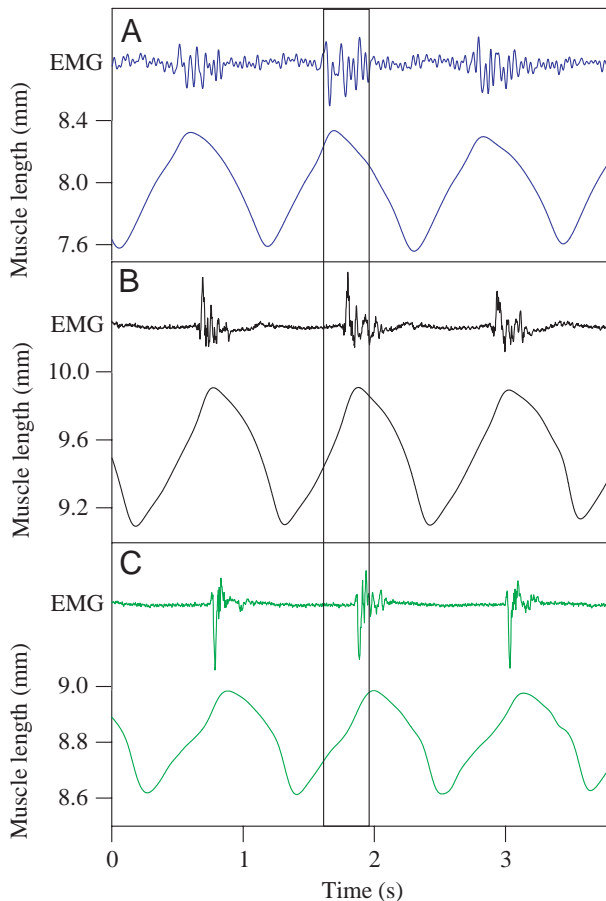


Fig. 9. EMG and sonometric data for three tailbeat cycles in an 88.0 cm leopard shark at three axial positions: anterior (A), mid (B) and posterior (C). The vertical lines indicate the phase of activation in the anterior axial position ($0.42 L$) and allow for comparison with the EMG/strain phases in the mid and posterior regions of the body.

of bending that travels from snout to tail during swimming, but the functional significance of this is unknown.

Interestingly, the phase of muscle activation, as well as the duty cycle, were similar along the body in the leopard shark. By contrast, all teleost species that have been examined display some degree of longitudinal variation in the phase of red muscle activation. This typically consists of (1) red muscle activation occurring relatively earlier in the strain cycle in more posterior locations (Williams et al., 1989; van Leeuwen et al., 1990; Rome et al., 1993; Wardle and Videler, 1993; Jayne and Lauder, 1995b; Gillis, 1998; Hammond et al., 1998; Shadwick et al., 1998; Ellerby and Altringham, 2001; Knowler et al., 1999) and (2) a decrease in the duration of muscle activation in more posterior locations (van Leeuwen et al., 1990; Rome et al., 1993; Wardle and Videler, 1993; Jayne and Lauder, 1995b; Gillis, 1998; Hammond et al., 1998; Shadwick et al., 1998; Ellerby and Altringham, 2001; Knowler et al., 1999). Because this negative phase shift in the timing of muscle activation is a common feature in most teleosts and is also seen in aquatic locomotion in eels (Gillis, 1998) and snakes (Jayne, 1988), Gillis (1998) proposed that this phase

shift may simply be a characteristic feature of axial-based undulatory swimming. However, our study shows that this is not the case in sharks like *Triakis* and therefore it does not appear to be a requirement for locomotion in cartilaginous fishes that swim by body-caudal fin propulsion.

Apparent differences between the pattern of red muscle activation in the leopard shark and most teleosts may reflect differences in the evolution of swimming in these two groups. Specifically, differential muscle function along the body, which occurs in many teleosts, may have evolved after the divergence of cartilaginous and bony fishes. In addition, many teleosts exhibit longitudinal differences in red muscle twitch kinetics that accompany differences in strain and activation patterns (Altringham and Ellerby, 1999). Given that there is no longitudinal variation in the EMG/strain phase relationship in the leopard shark, we hypothesize that the power-producing characteristics of the red muscle are also constant along the body in sharks that share a similar red muscle distribution. We are currently testing this hypothesis by performing *in vitro* work-loop studies. This will allow us to better understand differences in the mechanics of swimming and its evolution in bony and cartilaginous fishes.

We are grateful to C. Chan, E. Kisfaludy, C. Sepulveda and the Hubbs Sea World Research Facility for their assistance in shark collection, G. Lauder for providing software used in the body bending analysis, and J. Graham for the use of the swim tunnel. This research was supported by NSF IBN0091987 and a UC Regents Fellowship.

References

- Altringham, J. D. and Ellerby, D. J. (1999). Fish swimming: patterns in muscle function. *J. Exp. Biol.* **202**, 3397-3403.
- Altringham, J. D. and Johnston, I. A. (1990). Modelling muscle power output in a swimming fish. *J. Exp. Biol.* **148**, 395-402.
- Altringham, J. D. and Shadwick, R. E. (2001). Swimming and muscle function. In *Tuna Physiology, Ecology and Evolution* (ed. B. Block and D. E. Stevens), pp. 313-341. London: Academic Press.
- Altringham, J. D., Wardle, C. S. and Smith, C. I. (1993). Myotomal muscle function at different locations in the body of a swimming fish. *J. Exp. Biol.* **182**, 191-206.
- Bone, Q. (1966). On the function of the two types of myotomal muscle fibre in elasmobranch fish. *J. Mar. Biol. Assn UK* **46**, 321-349.
- Bone, Q., Kiceniuk, J. and Jones, D. R. (1978). On the role of the different fibre types in fish myotomes at intermediate swimming speeds. *Fish. Bull. USA* **76**, 691-699.
- Coughlin, D. J. and Rome, L. C. (1996). The roles of pink and red muscle in powering steady swimming in scup, *Stenotomus chrysops*. *Amer. Zool.* **36**, 666-677.
- Coughlin, D. J., Valdes, L. and Rome, L. C. (1996). Muscle length changes during swimming in scup: Sonomicrometry verifies the anatomical high-speed cine technique. *J. Exp. Biol.* **199**, 459-463.
- D'Aout, K. and Aerts, P. (1999). A kinematic comparison of forward and backward swimming in the eel *Anguilla anguilla*. *J. Exp. Biol.* **202**, 1511-1521.
- D'Aout, K., Curtin, N. A., Williams, T. L. and Aerts, P. (2001). Mechanical properties of red and white swimming muscles as a function of the position along the body of the eel *Anguilla anguilla*. *J. Exp. Biol.* **204**, 2221-2230.
- Ellerby, D. J. and Altringham, J. D. (2001). Spatial variation in fast muscle function of the rainbow trout *Oncorhynchus mykiss* during fast-starts and sprinting. *J. Exp. Biol.* **204**, 2239-2250.
- Ellerby, D. J., Altringham, J. D., Williams, T., and Block, B. A. (2000). Slow muscle function of pacific bonito (*Sarda chilensis*) during steady swimming. *J. Exp. Biol.* **203**, 2001-2013.

- Gillis, G.** (1998). Neuromuscular control of anguilliform locomotion: patterns of red and white muscle activity during swimming in the American eel *Anguilla rostrata*. *J. Exp. Biol.* **201**, 3245-3256.
- Graham, J. B., Dewar, H., Lai, N. C., Lowell, W. R. and Arce, S. M.** (1990). Aspects of shark swimming performance determined using a large water tunnel. *J. Exp. Biol.* **151**, 175-192.
- Greer-Walker, M.** (1970). Growth and development of the skeletal muscle fibers of the cod (*Gadus morhua*). *J. Cons. Perm. Int. Explor. Mar.* **33**, 228-244.
- Grillner, S. and Kashin, S.** (1976). On the generation and performance of swimming in fish. In *Neural Control of Locomotion* (ed. R. M. Herman, S. Grillner, P. S. G. Stein and D. G. Stuart), pp. 181-201. New York: Plenum Press.
- Hammond, L., Altringham, J. D. and Wardle, C. S.** (1998). Myotomal slow muscle function of rainbow trout *Oncorhynchus mykiss* during steady swimming. *J. Exp. Biol.* **201**, 1659-1671.
- He, P., Wardle, C. S. and Arimoto, T.** (1990). Electrophysiology of the red muscle of mackerel, *Scomber scombrus* and its relation to swimming at low speeds. In *The 2nd Asian Fisheries Forum* (ed. R. Hirano and I. Hanyu), pp. 469-472. Manila: Asian Fisheries Society.
- Hess, F. and Videler, J. J.** (1984). Fast continuous swimming of saithe (*Pollachius virens*): A dynamic analysis of bending movements and muscle power. *J. Exp. Biol.* **109**, 229-251.
- Hochachka, P. W., Hulbert, W. C. and Guppy, M.** (1978). The tuna power plant and furnace. In *The Physiological Ecology of Tunas* (ed. G. D. Sharp and A. E. Dizon), pp. 153-174. New York: Academic Press.
- Jayne, B. C.** (1988). Muscular mechanisms of snake locomotion: an electromyographic study of lateral undulation of the Florida Banded Water Snake (*Nerodia fasciata*) and the Yellow Rat Snake (*Elaphe obsoleta*). *J. Morph.* **197**, 159-181.
- Jayne, B. C. and Lauder, G. V.** (1993). Red and white muscle activity and kinematics of the escape response of the bluegill sunfish during swimming. *J. Comp. Physiol. A* **173**, 495-508.
- Jayne, B. C. and Lauder, G. V.** (1995a). Speed effects on midline kinematics during steady undulatory swimming of largemouth bass, *Micropterus salmoides*. *J. Exp. Biol.* **198**, 585-602.
- Jayne, B. C. and Lauder, G. V.** (1995b). Red muscle motor patterns during steady swimming in largemouth bass: Effects of speed and correlations with axial kinematics. *J. Exp. Biol.* **198**, 1575-1587.
- Johnson, T. P., Syme, D. A., Jayne, B. C., Lauder, G. V. and Bennett, A. F.** (1994). Modeling red muscle power output during steady and unsteady swimming in largemouth bass. *Am. J. Physiol.* **267**, R481-R488.
- Johnston, I. A. and Goldspink, G.** (1973a). A study of glycogen and lactate in the myotomal muscles and liver of the coalfish (*Gadus virens*) during sustained swimming. *J. Mar. Biol. Assn UK* **53**, 17-26.
- Johnston, I. A. and Goldspink, G.** (1973b). A study of the swimming performance of the Crucian carp *Carassius carassius* in relation to the effects of exercise and recovery on biochemical changes in the myotomal muscles and liver. *J. Fish Biol.* **5**, 249-260.
- Johnston, I. A., Davison, W. and Goldspink, G.** (1977). Energy metabolism of carp swimming muscles. *J. Comp. Physiol.* **114**, 203-216.
- Katz, S. L. and Shadwick, R. E.** (1998). Curvature of swimming fish midlines as an index of muscle strain suggests swimming muscle produces net positive work. *J. Theor. Biol.* **193**, 243-256.
- Knower, T., Shadwick, R. E., Katz, S. L., Graham, J. B. and Wardle, C. S.** (1999). Red muscle activation patterns in yellowfin and skipjack tunas during steady swimming. *J. Exp. Biol.* **202**, 2127-2138.
- Lindsay, C. C.** (1978). Form, function and locomotory habits in fish. In *Fish Physiology* (ed. W. S. Hoar and D. J. Randall), pp. 1-100. New York: Academic Press.
- Miller, D. J. and Lea, R. N.** (1972). Guide to Coastal Marine Fishes of California. *Fish Bulletin Number 157*, pp. 39. Sacramento: California Department of Fish and Game.
- Rayner, M. D. and Keenan, M. J.** (1967). Role of red and white muscles in the swimming of skipjack tuna. *Nature* **214**, 392-393.
- Rome, L. C., Funke, R. P. and Alexander, R. M.** (1990). The influence of temperature on muscle velocity and sustained performance in swimming carp. *J. Exp. Biol.* **154**, 163-178.
- Rome, L. C., Sosnicki, A. and Choi, I. H.** (1992). The influence of temperature on muscle function in the fast swimming scup. 2. The mechanics of red muscle. *J. Exp. Biol.* **163**, 281-295.
- Rome, L. C. and Swank, D.** (1992). The influence of temperature on power output of scup red muscle during cyclic length changes. *J. Exp. Biol.* **171**, 261-282.
- Rome, L. C., Swank, D. and Corda, D.** (1993). How Fish Power Swimming. *Science* **261**, 340-343.
- Shadwick, R. E., Katz, S. L., Korsmeyer, K. E., Knower, T. and Covell, J. W.** (1999). Muscle dynamics in skipjack tuna: timing of red muscle shortening in relation to activation and body curvature during steady swimming. *J. Exp. Biol.* **202**, 2139-2150.
- Shadwick, R. E., Steffensen, J. F., Katz, S. L. and Knower, T.** (1998). Muscle dynamics in fish during steady swimming. *Amer. Zool.* **38**, 755-770.
- Syme, D. A. and Shadwick, R. E.** (2002). Effects of longitudinal body position and swimming speed on mechanical power of deep red muscle from skipjack tuna (*Katsuwonus pelamis*). *J. Exp. Biol.* **205**, 189-200.
- van Leeuwen, J. L., Lankheet, M. J. M., Akster, H. A. and Osse, J. W. M.** (1990). Function of red axial muscles of carp (*Cyprinus carpio*): recruitment and normalized power output during swimming in different modes. *J. Zool.* **220**, 123-145.
- Wardle, C. S. and Videler, J. J.** (1993). The timing of the electromyogram in the lateral myotomes of mackerel and saithe at different swimming speeds. *J. Fish Biol.* **42**, 347-359.
- Wardle, C. S., Videler, J. J. and Altringham, J. D.** (1995). Tuning in to fish swimming waves: Body form, swimming mode and muscle function. *J. Exp. Biol.* **198**, 1629-1636.
- Webb, P. W.** (1975). Hydrodynamics and energetics of fish propulsion. *Bull. Fish. Res. Bd Can.* **190**, 1-159.
- Webb, P. W. and Keyes, R. S.** (1982). Swimming kinematics of sharks. *Fish. Bull.* **80**, 803-812.
- Williams, T. L., Grillner, S., Smoljaninov, V. V., Wallen, P., Kashin, S. and Rossignol, S.** (1989). Locomotion in lamprey and trout: the relative timing of activation and movement. *J. Exp. Biol.* **143**, 559-566.